THE WATER VAPOR ABUNDANCE IN ORION KL OUTFLOWS

José Cernicharo[2], Javier R. Goicoechea[3], Fabien Daniel[2],
Mercedes R. Lerate[4,5], Michael J. Barlow[5], Bruce M. Swinyard[4],
Ewine van Dishoeck[6], Tanya L. Lim[4], Serena Viti[5], Jeremy Yates[5]

Recieved 2006 May 17; accepted 2006 August 7; to be published in ApJ letters

ABSTRACT

We present the detection and modeling of more than 70 far–IR pure rotational lines of water vapor, including the ^{18}O and ^{17}O isotopologues, towards Orion KL. Observations were performed with the *Long Wavelength Spectrometer* Fabry–Perot (LWS/FP; $\lambda/\Delta\lambda \sim$6800-9700) on board the *Infrared Space Observatory* (ISO) between $\sim$43 and 197 μm. The water line profiles evolve from P–Cygni type profiles (even for the $H_2^{18}O$ lines) to pure emission at wavelengths above $\sim$100 μm. We find that most of the water emission/absorption arises from an extended flow of gas expanding at 25$\pm$5 km s^{-1}. Non–local radiative transfer models show that much of the water excitation and line profile formation is driven by the dust continuum emission. The derived beam averaged water abundance is 2–3$\times$10^{-5}. The inferred gas temperature T_k=80–100 K suggests that: (*i*) water could have been formed in the *plateau* by gas phase neutral-neutral reactions with activation barriers if the gas was previously heated (e.g. by shocks) to $\geq$500 K and/or (*ii*) H_2O formation in the outflow is dominated by *in–situ* evaporation of grain water–ice mantles and/or (*iii*) H_2O was formed in the innermost and warmer regions (e.g. the hot core) and was swept up in $\approx$1000 yr, the dynamical timescale of the outflow.

Subject headings: infrared: ISM: lines and bands—ISM: individual (Orion)—ISM: molecules—line: identification—radiative transfer

1. INTRODUCTION

Star forming regions are associated with violent phenomena such as cloud collapse, molecular outflows and related shocked regions. Under these conditions the neutral gas is warm and water vapor is predicted to be abundant (Draine & Roberge 1982) and to play a dominant role in the thermal balance (Neufeld & Kaufman 1993). Unfortunately, ground–based observations of H_2O are difficult and so the determination of water column densities is not straightforward. Nevertheless, ground–based observations of water maser lines have been performed toward Orion KL. From VLBI observations of the 6_{16}–5_{23} line at $\sim$22 GHz, Genzel et al. (1981) determined the kinematics and the expansion velocity for the so–called *low velocity outflow* ($\sim$18$\pm$2 km s^{-1}). The widespread nature of water vapor has been probed with maps of the 3_{13}–2_{20} line at $\sim$183 GHz (Cernicharo et al. 1990, 1994). This was the first time that the water abundance was estimated in the different large scale components around Orion KL. In addition, the high excitation conditions of the *plateau* gas (a mixture of outflows, shocks and interactions with the ambient cloud) has been revealed by observations of the 5_{15}–4_{22} line at $\sim$325 GHz (Menten et al. 1990; Cernicharo et al. 1999b). Due to their maser nature, the water abundance determination from these lines is quite involved. Even the observation of the $H_2^{18}O$ 3_{13}–2_{20} line at $\sim$203 GHz gives only poor estimates due to

the overlap with other molecular lines (Jacq et al. 1988). The HDO species has been also detected and modeled towards Orion KL (Jacq et al. 1990; Pardo et al. 2001), but the specific gas and dust chemistry has to be taken into account to derive χ(H_2O).

ISO (Kessler et al. 1996) spectrometers have provided the opportunity to observe many IR H_2O lines towards bright sources such as Orion KL. In particular, Harwitt et al. (1998) presented eight ISO/LWS/FP (Clegg et al. 1996) water lines between $\sim$71 and $\sim$125 μm involving energy levels between 300 and 800 K. They estimated χ(H_2O)$\simeq$5$\times$10^{-4}; however, the interpretation of these lines should include radiative pumping from IR dust photons. A larger set of weaker IR lines, including those of $H_2^{18}O$ and $H_2^{17}O$, is needed to minimize the opacity effects always associated with $H_2^{16}O$ lines. Orion KL has also been targeted with the *Short Wavelength Spectrometer* (SWS) tracing a smaller region than that probed by the LWS beam below $\sim$45 μm (van Dishoeck et al. 1998). Nineteen water absorption lines with energies between 200 and 750 K were detected (Wright et al. 2000). These authors suggested that mid–IR water lines arise from the *low–velocity outflow* and estimated χ(H_2O)=2–5$\times$10^{-4} (for an assumed gas temperature of 200–350 K). Most recently, the 1_{10}–1_{01} lines of $H_2^{16}O$ and $H_2^{18}O$ have been observed with SWAS (χ($H_2^{16}O$)$\simeq$3.5$\times$10^{-4}; Melnick et al. (2000); Snell et al. (2000)) and ODIN (χ($H_2^{16}O$)$\simeq$10^{-5}–10^{-4}; Olofsson et al. (2003)). In these observations, the $H_2^{16}O$ ground–state line shows widespread emission over a $\sim$5′ region.

In this letter we present all water lines detected in the first far–IR line survey towards Orion KL carried out with the ISO/LWS spectrometer (Lerate et al. 2006), and the radiative transfer models that fit the water data set (involving levels up to 2000 K).

[2] DAMIR, Instituto de Estructura de la Materia, Consejo Superior de Investigaciones Científicas, Serrano 121, 28006, Madrid, Spain. (cerni@damir.iem.csic.es)
[3] LERMA, UMR 8112, CNRS, Observatoire de Paris and Ecole Normale Supérieure, 24 Rue Lhomond, 75231 Paris 05, France.
[4] Rutherford Appleton Laboratory, Chilton, Didcot, UK.
[5] University College London, Gower Street, London WC13, UK.
[6] Sterrewacht Leiden, PO Box 9513, 2300 RA Leiden, The Netherlands.
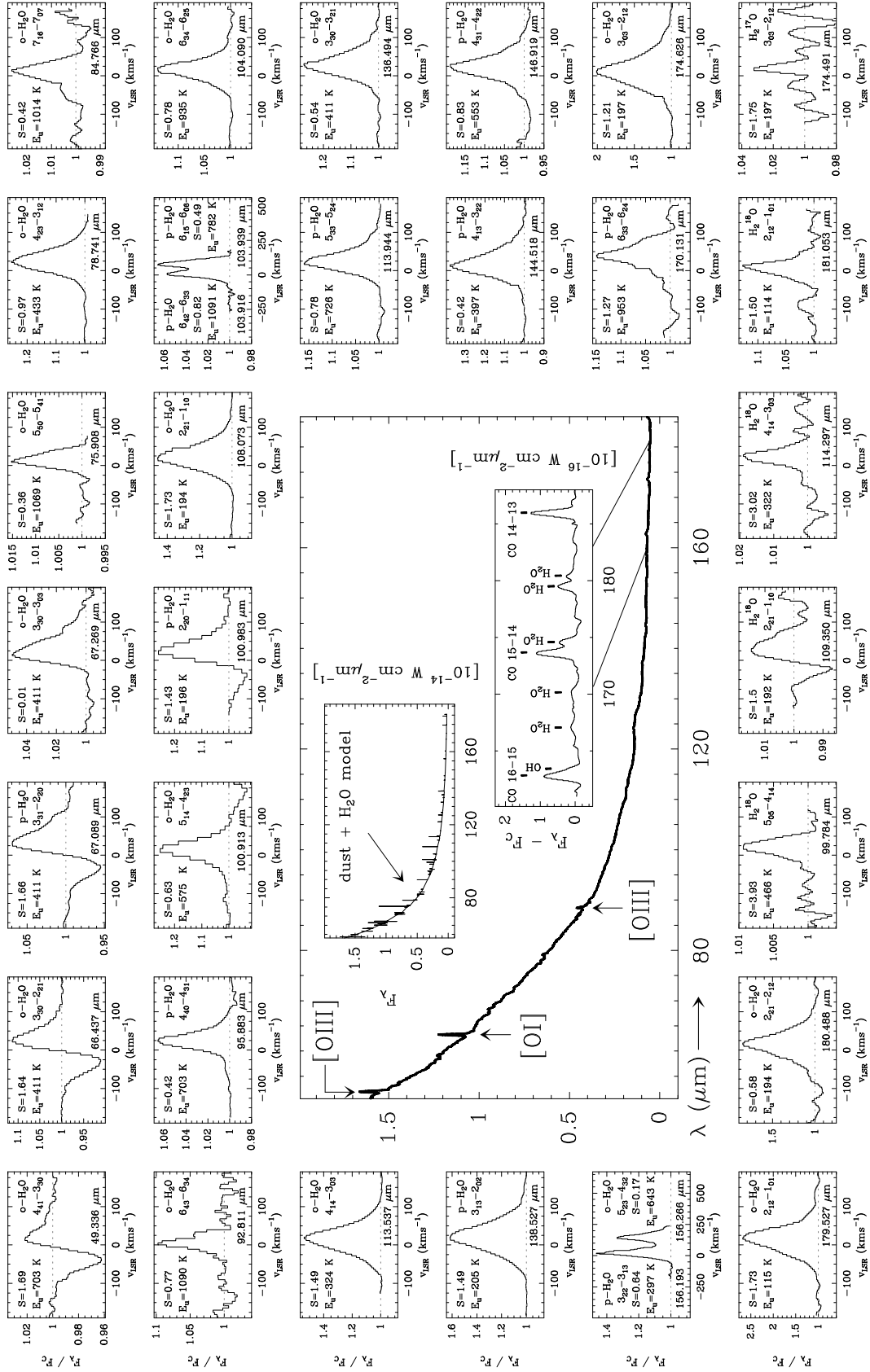
FIG. 1.— Summary of the 70 far–IR water lines detected by the ISO/LWS-FP towards Orion KL. The ordinate corresponds to the continuum normalized flux and the abscissa to the velocity (in km s^{-1}). Transition rotational numbers, rest wavelengths (in μm), upper level energies (in K) and intrinsic line strengths are shown in each box. The central inset shows the ISO/LWS-grating observations towards Orion at a resolution of $\lambda/\Delta\lambda \sim 300$. The ordinate corresponds to the absolute flux (in W cm^{-2} μm^{-1}) and the abscissa to the wavelength (in μm). Main molecular features between $\sim$160 and $\sim$197 μm are labelled in a zoom to the grating spectrum. The full radiative transfer model for the far–IR continuum and water line spectrum is also shown in the upper inset.

2. OBSERVATIONS AND DATA REDUCTION

All water lines within the range of the ISO/LWS ($\sim$43-197μm) were observed using long integrations with the FP spectrometer (L04 AOT) which provides the largest spectral resolution for the LWS instrument. Preliminary results were presented by Cernicharo et al. (1999a). In addition, a complete less sensitive (L03 AOT) far–IR line survey of Orion has been carried out. Adding both data sets more than 70 water lines have been detected (Lerate et al. 2006). The LWS circular aperture size is $\sim$80$''$, although it slightly depends on the particular LWS detector. In its FP mode the instrumental response is close to a broad–wing Lorentzian with a spectral resolution of $\lambda/\Delta\lambda$ $\sim$6800-9700. Processing of the water lines from AOT L03 was carried out using the Offline Processing (OLP) pipeline and the LWS Interactive Analysis (LIA) package version 10. AOT L04 spectra were analyzed using the ISO Spectral Analysis Package (ISAP[6]). The full description of the complex data calibration and reduction process and associated target dedicated time numbers, and all the tabulated line observations and spectroscopic parameters are given by Lerate et al. (2006).

3. RESULTS AND DISCUSSION

A summary of the resulting water lines is shown in Fig. 1. From these far–IR observations it is clear that water lines show a complicated behavior. For wavelengths above $\sim$100 μm, $H_2^{16}O$ lines are observed in emission. However, for shorter wavelengths, lines arising from energy levels below $\sim$1000 K and with large line–strengths, show P–Cygni profiles with emission covering a large velocity range. However, those with weak line-strengths or arising from higher energy levels, are observed in pure emission. $H_2^{18}O$ lines also show P–Cygni type profiles below $\sim$100 μm. In the $H_2^{18}O$ case, the absorption component is deeper than in the analogous $H_2^{16}O$ transition. Since optical depth effects are much less severe in $H_2^{18}O$ lines, the associated P–Cygni type profiles trace the main origin of far–IR water lines toward Orion KL, i.e. an extended outflow. Pure emission H_2O lines peak around $v \simeq 20$ km s^{-1} (the source v_{LSR} is $\sim$9 km s^{-1}; Scoville et al. 1993) but it is likely that the most opaque lines are redshifted due to self–absorption. On the other hand, water lines detected below $\sim$50 μm are observed in pure absorption with a velocity peak of $v \simeq -10$ km s^{-1} (the same applies to most water lines observed by ISO/SWS; Wright et al. (2000)).

The turnover point between absorption and emission lines is an important clue to interpret this large data set and to determine the relations between continuum+line opacity, line strengths, spatial distribution of gas, and physical conditions. ISO observations clearly show that most of the water vapor detected in the IR arises from a flow of gas expanding at 25$\pm$5 km s^{-1}. The inferred expansion velocity is consistent with the *low–velocity outflow* originally revealed by $\sim$22 GHz H_2O maser motions (Genzel et al. 1981), but a contribution from the extended *high–velocity outflow* could be present (Cernicharo et al. 1994). However, no high velocity line–wing emission is observed at ISO's sensitivity and S/N.

Similar conclusions have been found for the OH excited rotational lines (Goicoechea et al. 2006).

The main problem with modeling ISO data is the limited spatial resolution, which makes difficult to constrain the size and origin of the water region. Besides, any detailed fit to the data requires a detailed knowledge of the geometry and of the relative distribution of dust continuum and water lines. Fortunately, high angular resolution maps of water at $\sim$183 and $\sim$325 GHz lines do reveal the spatial and velocity distribution of water in Orion (Cernicharo et al. 1994, 1999b). In particular, Cernicharo and coworkers detected at least four different water components: the extended *ridge* (extended quiescent gas), the *plateau* (including the *high–* and *low–velocity outflows*) and the very narrow and strong features associated with the small water bullets observed at $\sim$22 GHz (Genzel et al. 1981). Besides, the newly detected far–IR water lines associated with the highest energy levels may have a contribution from the *hot core* (dense and hot inner regions). However, the large far–IR line–plus–continuum opacity will probably hide most of the *hot core* emission. Finally, radiative transfer effects in the most opaque lines, e.g. self–absorption and/or scattering by a lower density diffuse halo may possibly occur at velocity scales not resolved by ISO.

In order to estimate the water abundance, and the physical conditions prevailing in the expanding gas, we have modeled the first 30 rotational levels of both ortho– and para–H_2O using the same nonlocal code for lines and dust continuum as in the analysis of H_2O toward Sgr B2 (Cernicharo et al. 2006). The code has been described elsewhere (González-Alfonso & Cernicharo 1993) and has been recently improved to take into account a more sophisticated description of the dust emissivity and radiative transfer (Daniel et al. 2006, in prep.). The dust continuum emission has a crucial role in the radiative excitation of light species such as H_2O or OH with transitions in the far–IR and has to be correctly taken into account. In our model, level populations are consistently computed in statistical equilibrium considering collisional excitation and pumping by line and continuum photons. Collisional rates were scaled from those of H_2O–He collisions (Green et al 1993). A three–component model resembling the *hot core*, the *plateau* and the *ridge* is adopted. In this work we assume that most of the far–IR water lines arise only from the *plateau*. Of course, a minor contribution in the lowest excitation water lines may come from the more extended regions (producing narrow line emission) that we don't model here. A low water abundance of $(1–8)\times10^{-8}$ has been estimated in these regions from SWAS and ODIN observations (Snell et al. (2000); Olofsson et al. (2003)) and thus, the expected contribution to far–IR H_2O lines is small. In order to have the closest view of the IR radiation field seen by water vapor we have simultaneously tried to reproduce the full SWS/LWS/ISO continuum emission between $\sim$10 and $\sim$197 μm.

We find that the continuum level for $\lambda > 80$ μm is well reproduced by considering an inner 10$''$ IR continuum source (the *hot core*) simulated by a grey–body, with a color temperature of 200–250K, which is optically thick in the far–IR ($\tau_\lambda = 10 \times 150/\lambda$). The dust continuum emission from this *hot core* is attenuated
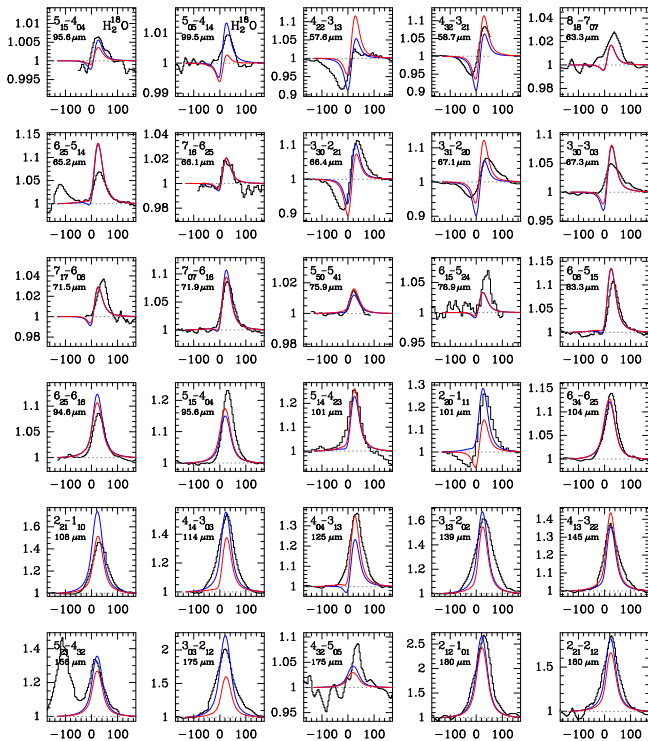
FIG. 2.— Radiative transfer model results discussed in the text. Selected synthetic line profiles (continuous curves) are shown over the observed ISO/LWS/FP detections (histograms). Model parameters are $\chi(H_2^{16}O)=3\times10^{-5}$, $n(H_2)=3.5\times10^5$ cm^{-3} and T_k=80 K (blue) and $\chi(H_2^{16}O)=2\times10^{-5}$, $n(H_2)=2.5\times10^5$ cm^{-3} and T_k=100 K (red). The ordinate corresponds to the continuum normalized flux and the abscissa to the velocity (in km s^{-1}). Synthetic line profiles have been convolved with a gaussian beam of 80$''$ and with a spectral resolution characterized by a Lorentzian with a width of 33 km s^{-1}.

by the surrounding components that we now describe. Taking into account the spatial extent of the 183 and 325 GHz water emission observed at higher spatial resolution (Cernicharo et al. 1990, 1994, 1999b), we model the *plateau* as a ∼40$''$ diameter unresolved shell expanding at 25±5 km s^{-1}, where water molecules and dust grains coexist (T_d=T_k is assumed). The radiative effects caused by an additional, only dust, 5$'$ diameter component (the *ridge*), with $T_d \simeq 25$ K and $n(H_2)\simeq10^5$ cm^{-3}, have been also included to fully match the SWS/LWS continuum level.

Dust absorption coefficients are computed from tabulated optical grain properties from Draine & Lee (1984), both in the *plateau* and in the *ridge*. Due to the large optical depth of $H_2^{16}O$ lines in the *plateau*, we have first modeled the $H_2^{18}O$ lines to obtain a more accurate estimate of the water abundance with less opacity constraint and faster level population convergence. A $^{16}O/^{18}O$ abundance ratio of 500 has been adopted. After a reasonable fit to the $H_2^{18}O$ lines, we iteratively search for the best physical conditions that enable to simultaneously reproduce the $H_2^{16}O$ and $H_2^{18}O$ spectra. Fig. 2 shows two representative models that qualitatively and quantitatively reproduce the majority of observed line profiles and intensities. The best models are found for a *plateau* temperature, density and water vapor abundance of T_k=80–100 K, $n(H_2)$=2.5–3.5×10^5 cm^{-3} and

$\chi(H_2^{16}O)$=2–3×10^{-5} respectively. The physical conditions inferred from water lines in the *plateau* are similar to those obtained from OH lines (Goicoechea et al. 2006), which suggests that far–IR lines from both species trace the same expanding gas. The derived water vapor abundance, $\gtrsim$2×10^{-5}, is obviously an averaged value over the large LWS/ISO beam and probably indicates that water can be locally more abundant, e.g. in the warmer interaction surfaces where the expanding gas shocks the dense ambient material. Larger angular resolution is needed to resolve the relative continuum and H_2O spatial distribution over this complex region. Nevertheless, the inferred gas temperatures, ∼100 K, are significantly below the gas temperature (∼300 K) required to activate the gas–phase neutral–neutral reactions converting most of the available oxygen into water (abundances larger than ∼10^{-4} are then predicted). Taken into account the short dynamical timescale of the outflow, ∼1000 years, water vapor could have been formed by these neutral–neutral reactions if the gas in the *plateau* was previously (or is locally) heated to ≥500 K, e.g. by a C–shock passage (Bergin et al. 1998). However, if the *plateau* gas temperature has reached a maximum temperature of only ∼100 K, other formation mechanisms are required to explain the observed water vapor abundances. In particular, the temperature inferred from ISO observations is similar to the water–ice evaporation temperature, and therefore, *in–situ* evaporation of water–ice grain mantles formed in an evolutionary stage prior to the onset of the outflow(s) could now dominate the water vapor formation in the *plateau*. Finally, the observed H_2O could have been also formed in the innermost and warmest regions (e.g. the hot core) and had been swept up by the outflow.

To conclude, despite the large number of detected far–IR excited water lines, neither high gas temperature nor high density conditions are required to populate the higher–energy water rotational levels. Radiative pumping due to the strong IR radiation field from the cloud is enough to populate these levels, at least in the average picture given by ISO observations. Future observations with *Herschel* will allow one to map many far–IR water resolved lines with improved angular resolution. It will then be possible to study in great detail the role of water in star forming regions.

REFERENCES

Bergin, E.A., Melnick, G.J, Neufeld, D.A. 1998, ApJ, 499, 777.

Blake, G. A., Sutton, E.C., Masson, C. R., & Phillips, T. G. 1987, ApJ, 315, 621.

Cernicharo, J., Thum, C., Hein, H., John, D., Garcia, P. & Mattioco, F. 1990, 231, L15

Cernicharo, J., González-Alfonso, E., E., Alcolea, J., Bachiller, R. & John, D. 1994, ApJ, 432, L59

Cernicharo J., et al. 1999a, The Universe as Seen by ISO. Eds. P. Cox & M. F. Kessler. ESA-SP 427., p. 565.

Cernicharo J., et al. 1999b, ApJ, 520, L131.

Cernicharo J., Goicoechea, J.R., Pardo, J.R., Asensio-Ramos, A. 2006, ApJ, 642, 940.

Clegg, P.E., et al. 1996, A&A, 315, L38

Draine, B. T., & Roberge, W. G. 1982, ApJ, 259, L91

Draine, B. T., & Lee, H.M. 1984, ApJ, 285, 89

Genzel, R., & Stutzki, J. 1989, ARA&A, 27, 41.

Genzel, R., Reid, M. J., Moran, J. M., & Downes, D. 1981, ApJ, 244, 884.

Goicoechea, et al. 2006, ApJ, 641, L49.

González-Alfonso, E. & Cernicharo, J. 1993, A&A, 279, 506.

Green, S., Maluendes, S., & McLean, A. D. 1993, ApJS, 85, 181

Harwit, M., Neufeld, D.A., Melnick, G.J., Kaufman, M.J. 1998, ApJ, 497, L105

Jacq, T., Henkel, C., Walmsley, C. M., Jewell, P. R. & Baudry, A. 1988, A&A, 199, L5

Jacq, T., Walmsley, C. M., Henkel, C., Baudry, A., Mauersberger, R. & Jewell, P. R. 1990, A&A, 228, 447

Kessler, M.F., et al. 1996, A&A, 315, L27

Menten, K.M., Melnick, G.J., Phillips, T.G., & Neufeld, D.A. 1990, ApJ, 363, L27

Melnick, G. J. et al. 2000, ApJ, 539, L87

Neufeld, D.A. & Kaufman, M.J. 1993, ApJ, 418, 263

Lerate, M.R. et al. MNRAS, 2006, 370, 597.

Liu, S.Y., Girart, J.M., Remijan, A. & Snyder, L. E. 2002, ApJ, 576, 255

Olofsson, A. O. H. et al. 2003, A&A, 402, L47.

Pardo, J.R., Cernicharo, J., Herpin, F., Kawamura, J., Kooi, J., & Phillips, T.G. 2001, ApJ, 562, 799

Snell, R.L. et al. 2000, ApJ, 539, L93

van Dishoeck, E. F. et al. 1998, ApJ502, L173

Wright, C.M. et al. 2000, A&A, 358, 689.

Wright, M. C. H., Plambeck, R. L. & Wilner, D. J. 1996, ApJ, 469, 216